Supplementary Information (SI) for Green Chemistry.
This journal is © The Royal Society of Chemistry 2026

Supporting Information

Multi-substrate conversion synchronous cofactor-regeneration for efficient natural product biosynthesis

Chaofeng Li, [a,b] Yeyun Wu, [c] Fei Gu, [c] Jiawei Wang, [a,b] Yicheng Xu, [d] Chao Liao, [a,b] Liangxu Liu, [a,b] Zhi Lin, [*a,b] and Jun Ni [*a,b,c]

[a.] State Key Laboratory of Microbial Metabolism, Joint International Research Laboratory of Metabolic & Developmental Sciences, and School of Life Sciences & Biotechnology, Shanghai Jiao Tong University, Shanghai 200240 (China).

[b.] Zhangjiang Institute for Advanced Study, Shanghai Jiao Tong University, Shanghai 201203 (China).

[c.] Innovation Center for Synthetic Biotechnology, Lumy Biotechnology, Changzhou, Jiangsu, 213200 (China).

[d.] School of Biotechnology, East China University of Science and Technology, Shanghai, 200237 (China).

Table of Contents

D. Supporting Tables

A. Materials and Methods

1. Chemicals and materials.

Raspberry ketone, (*R*)-rhododendrol and (*S*)-rhododendrol were purchased from Aladdin (Shanghai, China). 4-hy4-hydroxybenzylideneacetonedroxybenzylideneacetone was purchased from Yuanye Bio-Technology (Shanghai, China). The enzymes that were used for cloning of genes and construction of plasmids were purchased from New England Biolabs (restriction enzymes and DNA ligase) and Takara Biochemicals (DNA polymerase). All other chemicals were of analytical grade or chromatographically pure and were commercially available.

2. Plasmids, bacterial strains, and cultivation conditions.

The plasmids and bacterial strains used in this study are listed in Table S1 and S2. The *E. coli* BL21 (DE3) strains used for gene cloning and purification of enzymes were cultivated in Luria-Bertani (LB) broth medium: yeast extract (5 g), tryptone (10 g), and NaCl (10 g) in water (1 L, pH 7.0) containing appropriate antibiotics, at 200 rpm, 37 °C.

3. Gene prediction in *Albidovulum inexpectatum* and *Oceanicella* sp. SM1341.

The genes encoding raspberry ketone/zingerone synthase (RZS) were identified from the genomes of *Albidovulum inexpectatum* and *Oceanicella* sp. SM1341 based on BLAST of National Center for Biotechnology Information (NCBI) and previous reports on RZS in *Rubus idaeus*.[1] The multiple-sequence alignments of RZS were conducted using ClustalX 2.0, and phylogenetic trees were constructed using MEGA 7.0 and the neighbor-joining method.

4. Construction of recombinant plasmids.

All DNA manipulation and general molecular biology techniques were conducted according to the standard protocols. All plasmids and strains used in this study were listed in Table S1 and S2. The genes *Lk*ADH (WP_054768785.1)[2,3], *Ai*RZS (WP_104070788.1), *Oc*RZS (WP_118135018.1), *Am*ADH1E (XP_002928049.1), *Cs*ADH1E (XP_004431047.1), *Am*ADH1E^{4m} (*Am*ADH1E-D224A-I225R-N226S-D228R), *Cs*ADH1E^{4m} (*Cs*ADH1E-D224A-I225R-N226S-D228R), *Am*ADH1E^{m} (*Am*ADH1E-D224A), *Pa*ADH (NP 254114.1)[4], *Ni*CAR (QXN88043.1), *Bs*SFP (encoding phosphopantetheinyl transferase; AIY95948.1)[5] *Aa*ADH (WP_011237618.1)[6] and *Gt*ALDH (WP_011888257.1, W173M)[7] were codon optimized for *E. coli* expression and synthesized by a synthetic DNA service provider (Genscipt Biotechnology Inc.). The vector pETDuet-1 was double digested with *Bam*HI and *Not*I, afterwards, the genes *Lk*ADH, *Ai*RZS, *Oc*RZS, *Am*ADH1E, *Cs*ADH1E, *Am*ADH1E^{4m}, or *Am*ADH1E^{m} was cloned into the *Bam*HI-NotI sites of pETDuet-1, respectively, to generate pET-*Lk*ADH, pET-*Ai*RZS, pET-*Oc*RZS, pET-*Am*ADH1E, pET-*Cs*ADH1E, pET-*Am*ADH1E^{4m}, pET-*Cs*ADH1E^{4m}, or pET-*Am*ADH1E^{m} for the expression and purification of the specific enzyme. The genes *Pa*ADH, *Ni*CAR, *Bs*SFP, *Aa*ADH and *Gt*ALDH was cloned into pRSFDuet-1, respectively, to generate pRSF-*Pa*ADH, pRSF-*Ni*CAR, pRSF-*Bs*SFP, pRSF-*Aa*ADH and pRSF-*Gt*ALDH for the expression and purification of the specific enzyme.

5. Purification of the recombinant enzymes.

To express *Lk*ADH, *Ai*RZS, *Oc*RZS, *Am*ADH1E, *Cs*ADH1E, *Am*ADH1E^{4m}, *Cs*ADH1E^{4m}, and *Am*ADH1E^{m}, the recombinant strains were cultured at 37 °C, and when the growth of recombinant *E. coli* reached OD_{600}=0.6, 0.2 mM IPTG were add to induce the expression of heterologous genes. The cells were washed with PBS after induction for 12-16 h, then resuspended with binding buffer (25 mM Tris-HCl, pH 8.0, 300 mM NaCl, 20 mM imidazole) to OD_{600}=30. Crude cell extracts were prepared by ultrasonic sound, and before that protease inhibitor phenylmethanesulfonyl fluoride (PMSF) was added to the cell suspensions at a final concentration of 1 mM. After centrifugation (12000 rpm, 30 min), the supernatant containing soluble protein fraction was obtained, then used for affinity purification by Ni-NTA column. The target proteins were eluted by elution buffer (25mM Tris-HCl, pH 8.0, 300 mM NaCl, 300 mM imidazole), and were transferred to Amicon Ultra - 15 30 K Centrifugal Filter Devices (Merck Millipore, Germany) for further diafiltration, buffer exchange and protein concentration. Purified proteins were obtained at last, quantified according to the Bradford method, and confirmed by SDS-PAGE. All the purification process was performed at 4 °C to ensure the enzyme activity, and the purified enzymes were stored at -80 °C for further experiments.

6. Activity assay of the enzymes *Lk*ADH, *Ai*RZS, *Oc*RZS, *Am*ADH1E, *Cs*ADH1E, *Am*ADH1E^{4m}, and *Am*ADH1E^{m}.

*Lk*ADH activity was assayed according to the previous research. The catalytic activitiy of *Lk*ADH for (*R*)-rhododendrol was determined with the purified enzyme. The reaction mixture (200 μL) contained 15 μM purified enzyme, $NADP^+$ (1 mM) and substrate (1 mM) in Glycine-NaOH with Mg^{2+} buffer (pH 9.0). The reaction was performed for 30 min, after which 15 μL 8 M HCl was added to stop the reaction.

The optimum temperature and pH of *Lk*ADH were determined according to the above method. The temperature ranged from 35 °C to 55 °C, and the mixture was shaken vigorously for 30 min. Then, the optimum pH was tested for pH values ranging from 7.0 to 10.5 at 40 °C using different pH buffer solutions. Each experiment was run in triplicate. The catalytic activity of *Lk*ADH for converting (*R*)-rhododendrol was identified by HPLC analysis.

The catalytic activity of *Ai*RZS for 4-Hydroxybenzylideneacetone was determined with the purified enzyme. The reaction mixture (200 μL) contained 1.5 μM purified enzyme, NADPH (1 mM) and substrate (1 mM) in HEPES buffer (pH 7.0). The reaction was performed for 15 min at 45 °C, after which 15 μL 8 M HCl was added to stop the reaction.

The optimum temperature of *Ai*RZS and *Oc*RZS were determined with these purified enzymes. The reaction mixture (200 μL) contained 1.5 μM purified enzyme, NADPH (1 mM) and substrate (1 mM). The temperature ranged from 30 °C to 90 °C, and the mixture was incubated in HEPES buffer (pH 7.0) for 15 min. Then, the optimum pH of *Ai*RZS was tested for pH values ranging from 4.0 to 10.5 at 45 °C using different pH buffer solutions. Each experiment was run in triplicate. The catalytic activities of *Ai*RZS and *Oc*RZS for converting 4-Hydroxybenzylideneacetone were identified by HPLC analysis.

The optimum temperature and pH of *Am*ADH1E, *Cs*ADH1E, and *Am*ADH1E^{m} were determined with these purified enzymes. The reaction mixture (200 μL) contained 2.5 μM purified enzyme, $NADP^+$ (1 mM) and substrate (1 mM). The temperature ranged from 20 °C to 80 °C, and the mixture was incubated in HEPES buffer (pH 7.0) for 30 min. Then, the optimum pH was tested for pH values ranging from 4.0 to 10.5 at optimum temperature (AmADH1E, 70 °C; CsADH1E, 60 °C) using different pH buffer solutions. Each experiment was run in triplicate. The catalytic activities of *Am*ADH1E, *Cs*ADH1E, and *Am*ADH1E^{m} for converting (*S*)-rhododendrol were identified by HPLC analysis.

The cofactor preference of *Am*ADH1E, *Cs*ADH1E, *Am*ADH1E^{4m} and *Am*ADH1E^{m} were determined by adding different cofactors. The reaction mixture (200 μL) contained 2.5 μM purified enzyme, $NADP^+$ or NAD^+ (1 mM) and substrate (1 mM) in HEPES buffer (pH 7). The reaction was performed for 30 min at 40 °C, after which 15 μL 8 M HCl was added to stop the reaction. Each experiment was run in triplicate.

7. Raspberry ketone production by MSCR strategy.

The *Lk*ADH/*Ai*RZS MSCR system was used to convert (*R*)-rhododendrol and 4-HBA into raspberry ketone. The reaction mixture (200 μL) contained 1 mM substrate (0.5 mM (*R*)-rhododendrol, 0.5 mM 4-HBA), 30 μM *Lk*ADH and 1.5 μM *Ai*RZS, with sufficient cofactors (1 mM NADPH and 1 mM $NADP^+$) or sub-stoichiometric cofactors (0.02/0.1 mM $NADP^+$). The reaction was performed for 30 min in Glycine-NaOH with Mg^{2+} buffer (pH 9.0) at 40 °C, after which 15 μL 8 M HCl was added to stop the reaction.

The *Am*ADH1E^{m}/*Ai*RZS MSCR system was used to covert (*S*)-rhododendrol and 4-HBA into raspberry ketone. The reaction mixture (200 μL) contained 1 mM substrate (0.5 mM (*S*)-rhododendrol, 0.5 mM 4-HBA), 2.5 μM *Am*ADH1E^{m} and 1.5 μM *Ai*RZS, with sufficient cofactors (1 mM NADPH and 1 mM $NADP^+$) or sub-stoichiometric cofactors (0.02/0.1 mM $NADP^+$). The reaction was performed for 30 min in Glycine-NaOH with Mg^{2+} buffer (pH 9.0) at 40 °C, after which 15 μL 8 M HCl was added to stop the reaction.

The *Lk*ADH/*Am*ADH1E^{m}/*Ai*RZS MSCR system was used to convert (*R*) and (*S*)-rhododendrol and 4-HBA into raspberry ketone. The reaction mixture (200 μL) contained 1 mM substrate (0.5 mM racemic-rhododendrol, 0.5 mM 4-HBA), 18 μM *Lk*ADH, 3 μM *Am*ADH1E^{m} and 1.5 μM *Ai*RZS, with sufficient cofactors (1 mM NADPH and 1 mM $NADP^+$) or sub-stoichiometric cofactors (0.02/0.1 mM $NADP^+$). The reaction was performed for 15 min in Glycine-NaOH with Mg^{2+} buffer (pH 9.0) at 40 °C, after which 15 μL 8 M HCl was added to stop the reaction. When conducting response surface experiments, the amount of *Ai*RZS was set at 1.5 μM, the amount of *Lk*ADH was set at 6~22.5 μM, and the amount of *Am*ADH1E^{m} was set at 1.5~6 μM, with sufficient cofactors (1 mM NADPH and 1 mM $NADP^+$). The reaction was performed for 15 min in Glycine-NaOH with Mg^{2+} buffer (pH 9.0) at 40 °C, after which 15 μL 8 M HCl was added to stop the reaction.

8. Cinnamaldehyde production by MSCR strategy.

The *Pa*ADH/*Ni*CAR/*Bs*SFP MSCR system was used to convert cinnamyl alcohol and cinnamic acid into cinnamaldehyde. The reaction mixture (200 μL) contained 1 mM substrate (0.5 mM cinnamyl alcohol, 0.5 mM cinnamic acid), the amount of *BsSFP* was set at 2 μM, the amount of *Ni*CAR was set at 2~4 μM, and the amount of *Pa*ADH was set at 4~12 μM, with sufficient cofactors (1 mM NADPH and 1 mM $NADP^+$) or sub-stoichiometric cofactors (0.1 mM $NADP^+$). The reaction was performed for 30 min in Tris·HCl buffer (pH 8.0) at 40 °C, after which 15 μL 8 M HCl was added to stop the reaction.

9. Benzaldehyde production by MSCR strategy.

The *Aa*ADH/*Gt*ALDH MSCR system was used to convert benzyl alcohol and benzoic acid into benzaldehyde. The reaction mixture (200 μL) contained 1 mM substrate (0.5 mM benzyl alcohol, 0.5 mM benzoic acid), the amount of *Aa*ADH was set at 2~4 μM, and the amount of *Gt*ALDH was set at 2~4 μM, with cofactors (0.5 mM NADH and 0.5 mM NAD^+), The reaction was performed for 2 hours in phosphate buffer (pH 7.5) at 30 °C, after which 15 μL 8 M HCl was added to stop the reaction.

10. Analysis and quantification of products.

For HPLC analysis, the samples were centrifuged at 12000 rpm, for 10 min and the supernatants were filtered using 0.2 μm syringe filter. HPLC analysis was performed using an Agilent 1260 Infinity II instrument with an Eclipse Plus-C18 column (2.1× 50 mm) and an Ultimate 3000 Photodiode Array Detector maintained at 30 °C. The substrate and product were analyzed by using the following method. The flow rate was 0.5 mL/min and the mobile phase consisted of 80 % solvent A (0.1% phosphoric acid in water) and 20 % solvent B (acetonitrile). Rhododendrol and raspberry ketone were monitored by measuring the absorbance at 192 nm. 4-Hydroxybenzylideneacetone was monitored by measuring the absorbance at 310 nm. Cinnamyl alcohol, cinnamic acid and cinnamaldehyde were monitored by measuring the absorbance at 254 nm. Benzyl alcohol, benzoic acid and benzaldehyde were monitored by measuring the absorbance at 230 nm. For cinnamaldehyde and benzaldehyde analysis, the mobile phase was adjusted to 50 % solvent A (0.1% phosphoric acid in water) and 50 % solvent B (acetonitrile). After separation by HPLC, LC-MS/MS analysis was conducted using a Shimadzu Corporation LC-MS/MS-8045 system for the examination of products. The ion mass spectrometry data for the standard compounds were recorded as follows: raspberry ketone at m/z = 163.2, cinnamaldehyde at m/z = 133.1, benzaldehyde at m/z = 104.95 (Figure S7).

11. Calculation of carbon atom conversion rate.

In this study, the carbon atom conversion rate is defined as the percentage of carbon atoms from all substrates that are retained in the target product, calculated based on the molar ratio of carbon atoms before and after the reaction. This metric reflects the efficiency of converting substrate carbon atoms into the target product.

The carbon atom conversion rate based on MSCR strategy is calculated as follows:

Carbon atom conversion rate (%) = (Moles of carbon atoms in the product / Total moles of carbon atoms in all substrates) ×100%

Example calculation carbon atom conversion rate (for **raspberry ketone** synthesis):

In the MSCR system, the substrates are rhododendrol (RD, $C_{10}H_{14}O_2$, containing 10 carbon atoms) and 4-hydroxybenzylideneacetone (4-HBA, $C_{10}H_{10}O_2$, containing 10 carbon atoms). The target product, raspberry ketone (RK, $C_{10}H_{12}O_2$), also contains 10 carbon atoms. Since the redox reactions described involve no loss or gain of carbon atoms, each substrate molecule is converted into one molecule of the target product with the same carbon skeleton.

Total substrate loading was 1 mM (consisting of 0.5 mM RD and 0.5 mM 4-HBA), corresponding to a total of 10 mM of carbon atoms:

Total moles of carbon atoms in all substrates = 0.5 mM RD × 10 (Carbon number) + 0.5 mM 4-HBA × 10 (Carbon number) = 10 mM.

The quantified raspberry ketone concentration was 155.47 mg/L, and the molecular weight of RK is 164.204 g/mol. Thus, the moles of carbon atoms in the product were calculated as:

Moles of carbon atoms in the product = (155.47 mg/L) / (164.204 g/mol) RK × 10 (Carbon number) = 9.468 mM.

Therefore:

Carbon atom conversion rate (%) = (9.468 mM / 10 mM) × 100% = 94.68%.

B. Supporting Discussion

Discussion on industrial optimization of the MSCR strategy.

As a proof-of-concept prototype, the MSCR strategy couples oxidation and reduction reactions for natural product biosynthesis, enabling bidirectional recycling of redox cofactors to maintain redox balance without sacrificing agents. However, several practical aspects require further optimization for subsequent industrial application.

1. Productivity and cost-effectiveness.

Current product titers remain moderate for direct industrial application. Future efforts should focus on enzyme immobilization and enzyme engineering (e.g., directed evolution or AI-driven design) to enhance catalytic efficiency and stability, as well as reactor and process optimization to improve productivity. Cost-effectiveness may be a key challenge for the industrial scale-up of these purified enzymes reactions. Recently, numerous efforts have been made to remove cost barriers in industrial enzymes manufacturing, such as enzyme immobilization techniques, [8-13] reactor optimization,[14, 15] and process optimization.[16, 17] Enzyme immobilization is widely regarded as one of the most effective methods to reduce production costs. By fixing or entrapping enzymes within solid support materials, immobilization strategies can improve enzyme stability and reusability, thereby reducing enzyme consumption and lowering overall production cost.[8-10] Reactor technologies and process optimization are critical aspects ensuring efficient reaction between substrate and enzymes, which is essential for making enzyme production systems more efficient, cost-effective, and sustainable.[14-17] In addition, cell lysate-based catalysis offers a cost-effective alternative. However, the use of lysates for redox reactions may present certain challenges. The MSCR strategy generally aims to synthesize aldehydes and ketones by combining oxidation and reduction reactions, and these molecules are vulnerable to metabolism by more than ten endogenous alcohol dehydrogenases (ADHs) and aldo-keto reductases (AKRs) with broad substrate specificity in many microorganisms.[18-25] Therefore, the use of crude lysate may introduce interference from endogenous ADHs and AKRs, potentially affecting cofactor balance or leading to side reactions. To eliminate redundant endogenous enzymes, future efforts may involve optimizing the host strain background (i.e., deleting endogenous ADHs and AKRs) or implementing lysate pretreatment to minimize such interference.

2. Enzyme activity and stability.

Enzyme stability is critical to their potential for industrial application. Contemporary enzyme screening has evolved into a systematic workflow integrating bioinformatics prediction, automated library construction, and high-throughput screening.[26-29] Following screening, the optimal enzyme variants undergo reaction condition optimization to identify their ideal working environment, thereby paving the way for subsequent industrial application. To further improve enzyme stability and activity, several strategies can be employed. First, enzyme immobilization on solid support materials enhances reusability and thermal stability while reducing production costs.[30-33] Second, structure modification through directed evolution, rational design, or semi-rational design can significantly improve thermostability, such as introducing non-covalent interactions and cyclization.[34-38] Third, chemical modification (e.g., crosslinked enzyme crystals) offers additional alternative.[30, 39, 40] Furthermore, interface modification engineering is effective for multimeric enzymes,[41] and when pH compatibility issues arise between enzymes, approaches like site-directed mutagenesis or fusion enzyme design can align their pH adaptability.[42, 43] With the advancement of AI-driven tools such as AlphaFold and protein language models (e.g., Evolutionary scale modelling),[44-46] the prediction and enhancement of enzyme properties are becoming more efficient, opening new avenues for industrial biocatalysis.

3. Substrate scope and downstream processing.

By combining different oxidation modules with reduction modules, this strategy holds great potential for synthesizing a wide variety of valuable natural products from diverse redox precursors, such as dihydrocarvone,[47, 48] menthone,[49, 50] *p*-hydroxybenzaldehyde,[7, 51] geranial,[7, 52] coniferyl aldehyde,[7, 53] *p*-coumaraldehydea,[7, 54] veratraldehyde,[55, 56] sinapaldehyde,[57, 58] caffeyl aldehyde,[59, 60] and leucocyanidin[61] (Figure S8). In this study, the MSCR strategy (convergent cascades) is designed to converge these oxidized and reduced precursors toward a common intermediate product, thereby greatly facilitating downstream separation and purification process. Coupling substrates to generate different final products is theoretically feasible and represents an interesting direction for future exploration. For example, by coupling the oxidation of cinnamyl alcohol to cinnamaldehyde with the reduction of protocatechuic acid into gallic acid, simultaneously generating two distinct valuable compounds cinnamaldehyde and gallic acid, Using the same approach, by combining different oxidation modules with reduction module, the “non-convergent cascades” holds great potential for synthesizing a wide variety of valuable natural products. However, generating different final products introduces additional complexity in downstream separation and purification process. The choice of separation method should be tailored to the

specific product pair based on their distinct physicochemical properties, including polarity, volatility, and solubility. Approaches such as liquid–liquid extraction, chromatographic separation, capillary electrophoresis, or resin-based adsorption can be selected on a case-by-case basis. For example, one product is preferentially soluble in the aqueous phase (i.e., gallic acid) while the other partitions into an organic phase (i.e., cinnamaldehyde), allowing straightforward separation by liquid–liquid extraction, enabling one-pot cascade biosynthesis with in situ product purification.

C. Supporting Figures

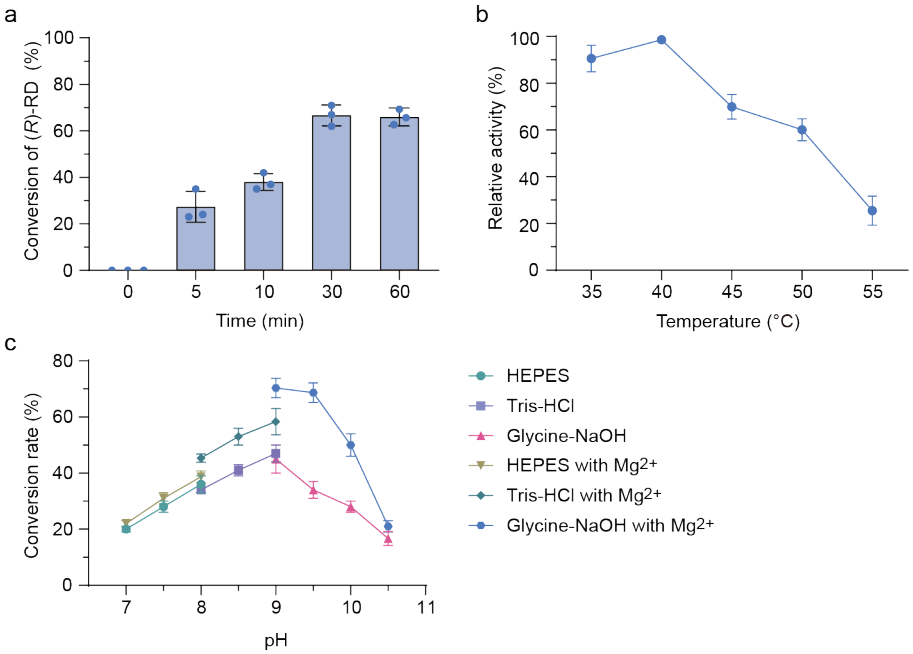

Figure S1. Biotransformation of (*R*)-RD to RK and characterization of *Lk*ADH activity. (a) Biotransformation of (*R*)-RD to RK by *Lk*ADH. (b) Effects of temperature on *Lk*ADH activity. (c) Effects of pH on the conversion rate of *(R)*-RD to RK catalyzed by *Lk*ADH.

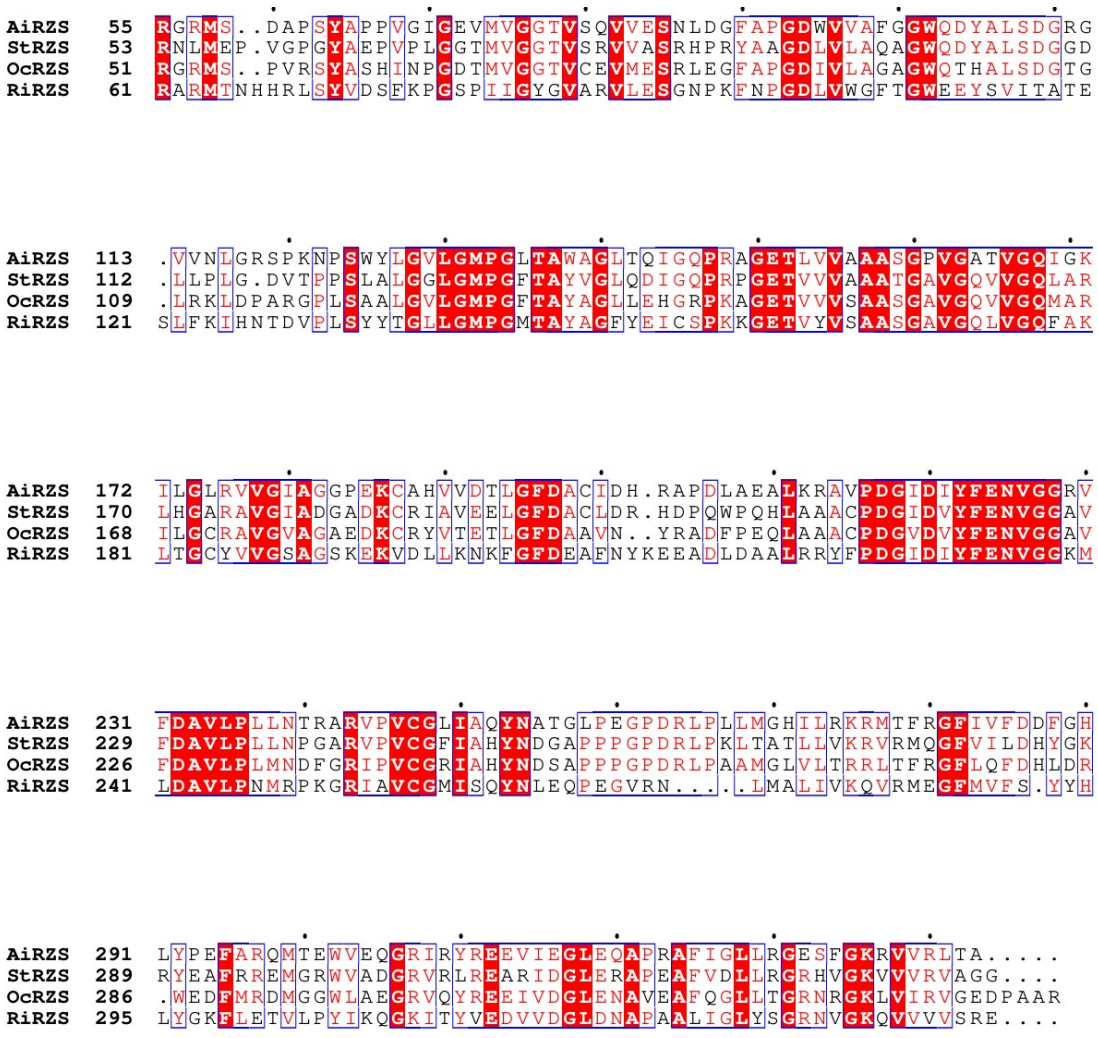

Figure S2. Multiple alignment of the amino acid sequences of raspberry ketone/zingerone synthase (RZS). Identical residues are shaded in red.

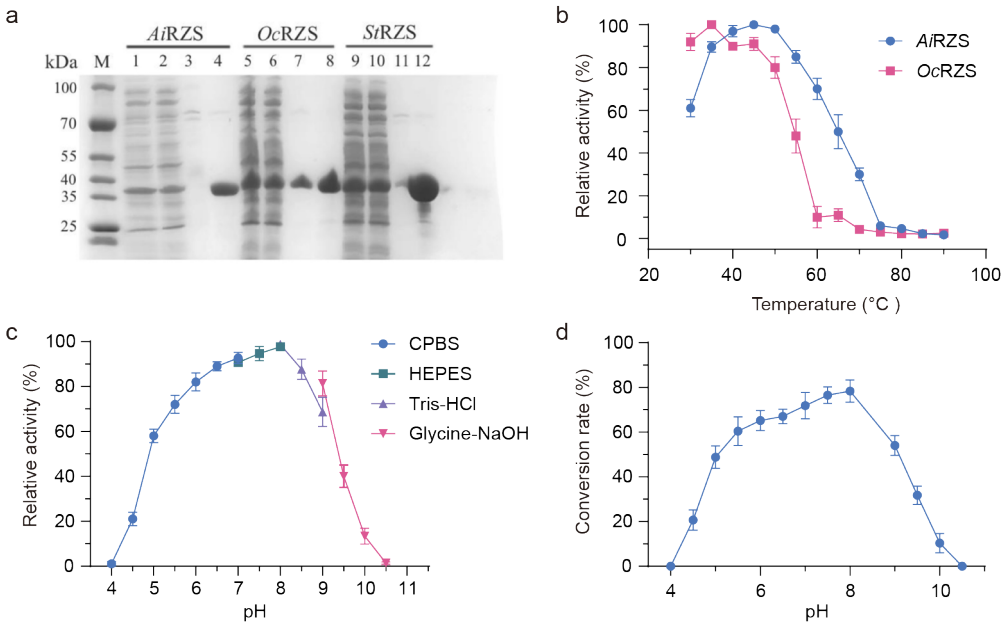

Figure S3. Purification and enzymatic characterization of RZS. (a) SDS-PAGE gel electrophoresis of the purified *Ai*RZS, *Oc*RZS and *St*RZS. Lane M, protein marker (Fermentas Canada Inc., Burlington, Canada); lane 1, 5 and 9, cell extract of recombinant *E. coli* BL21 (DE3) strain; lane 2, 6 and 10, supernatant of induced cell lysate; lane 3, 4, 7, 8 11 and 12, purified protein eluted with varying imidazole concentrations. Molecular mass is indicated at the left of the figure. (b) Effects of temperature on *Ai*RZS and *Oc*RZS activity. (c) Effects of pH on *Ai*RZS relative activity and (d) catalytic efficiency.

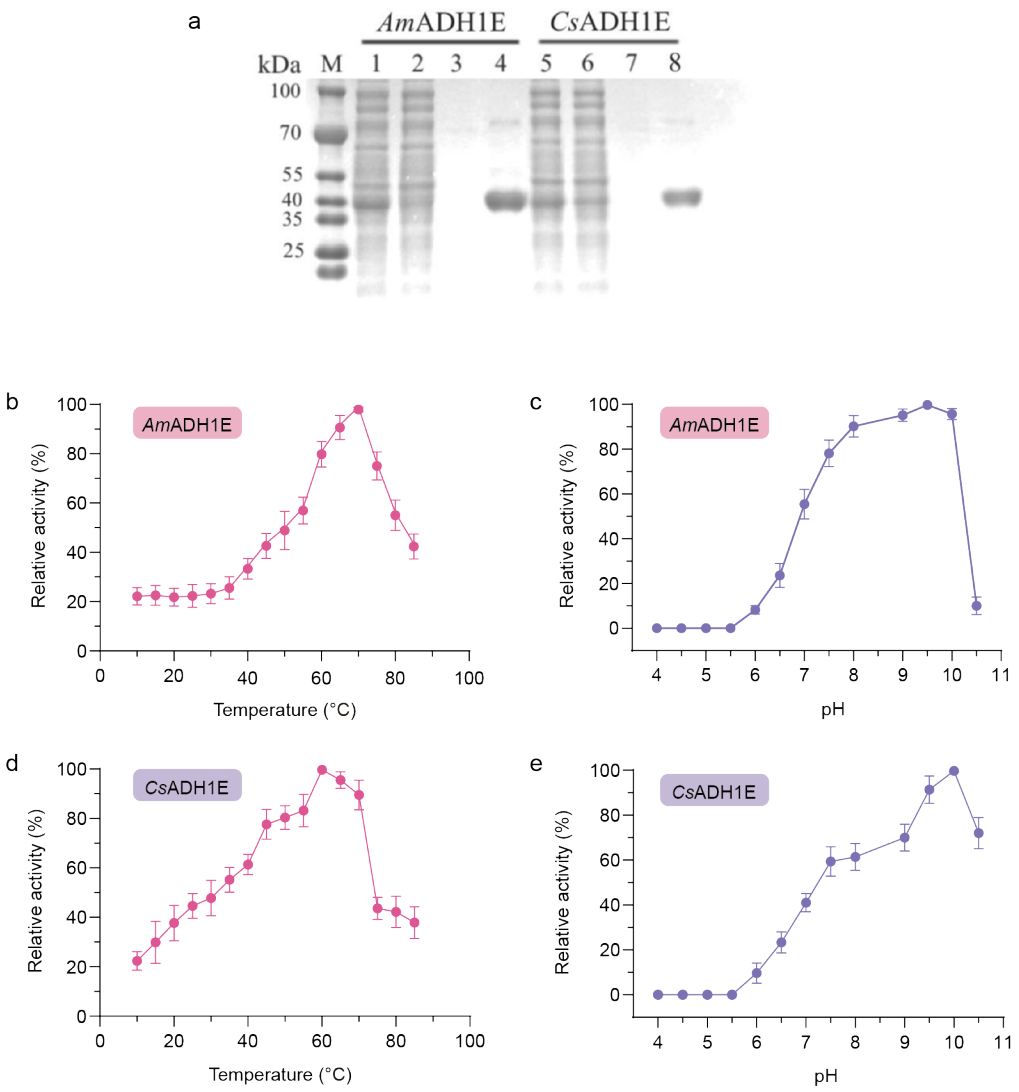

Figure S4. Purification and enzymatic characterization of *Am*ADH1E and *Cs*ADH1E. (a) SDS-PAGE gel electrophoresis of the purified *Am*ADH1E and *Cs*ADH1E. Lane M, protein marke; lane 1 and 5, cell extract of recombinant *E. coli* BL21 (DE3) strain; lane 2 and 6, supernatant of induced cell lysate; lane 3, 4, 7 and 8, purified protein eluted with varying imidazole concentrations. Molecular mass is indicated at the left of the figure. Effects of temperature (b) and pH (c) on *Am*ADH1E activity. Effects of temperature (d) and pH (e) on *Cs*ADH1E activity.

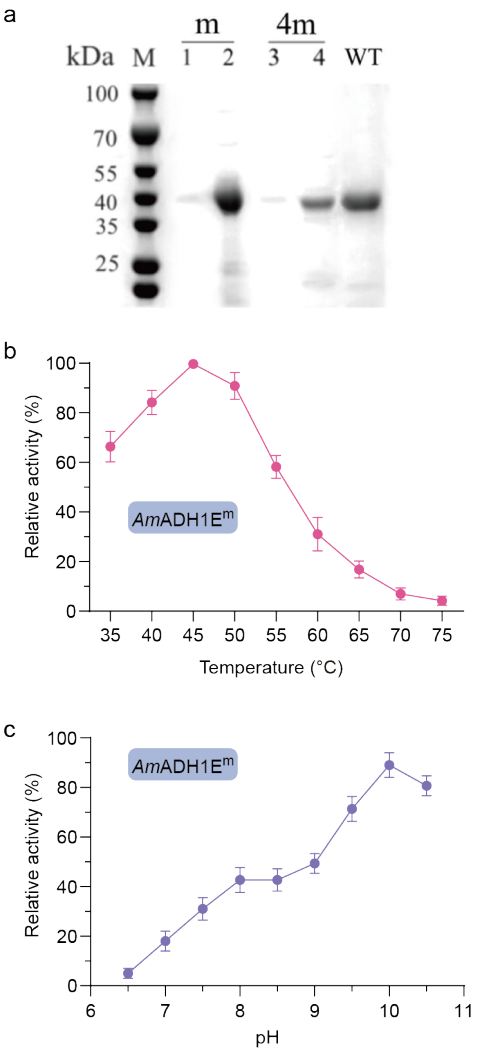

Figure S5. Purification and enzymatic characterization of *Am*ADH1E^{m}. (a) SDS-PAGE gel electrophoresis of the purified *Am*ADH1E^{m} (m) and *Am*ADH1E4^{m} (4m). Lane M, protein marker; lane 1, 2, 3 and 4, purified protein eluted with varying imidazole concentrations. Wild type (WT) as control. Molecular mass is indicated at the left of the figure. (b) Effects of temperature on AmADH1E^{m} relative activity. (c) Effects of pH on AmADH1E^{m} relative activity.

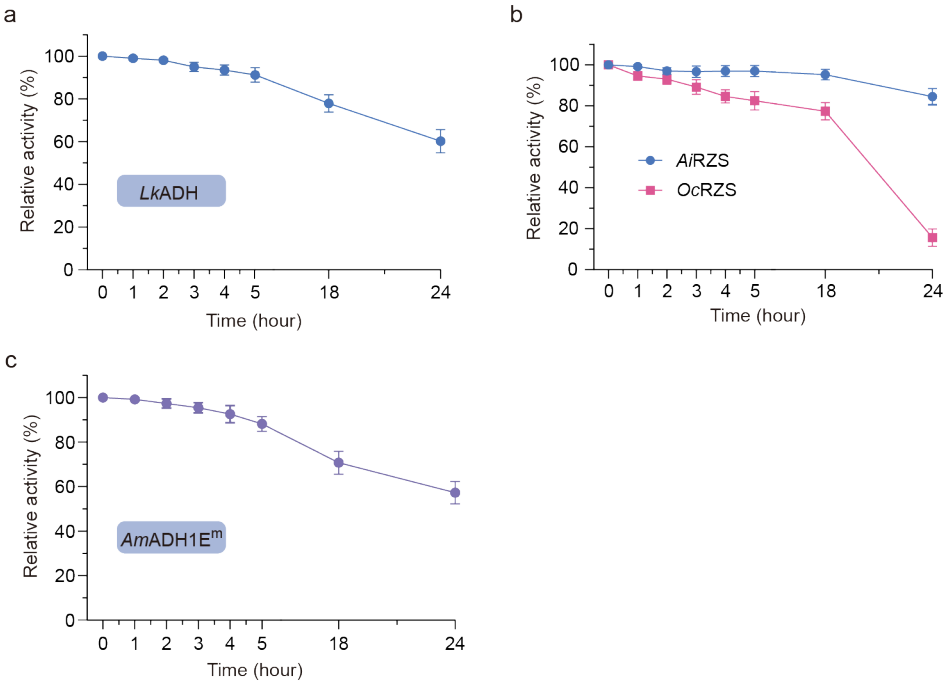

Figure S6. Time-activity profiles of enzyme (a) *Lk*ADH, (b) *Ai*RZS and *Oc*RZS, (c) *Am*ADH1E^{m} at pH 9.0 and 40 °C.

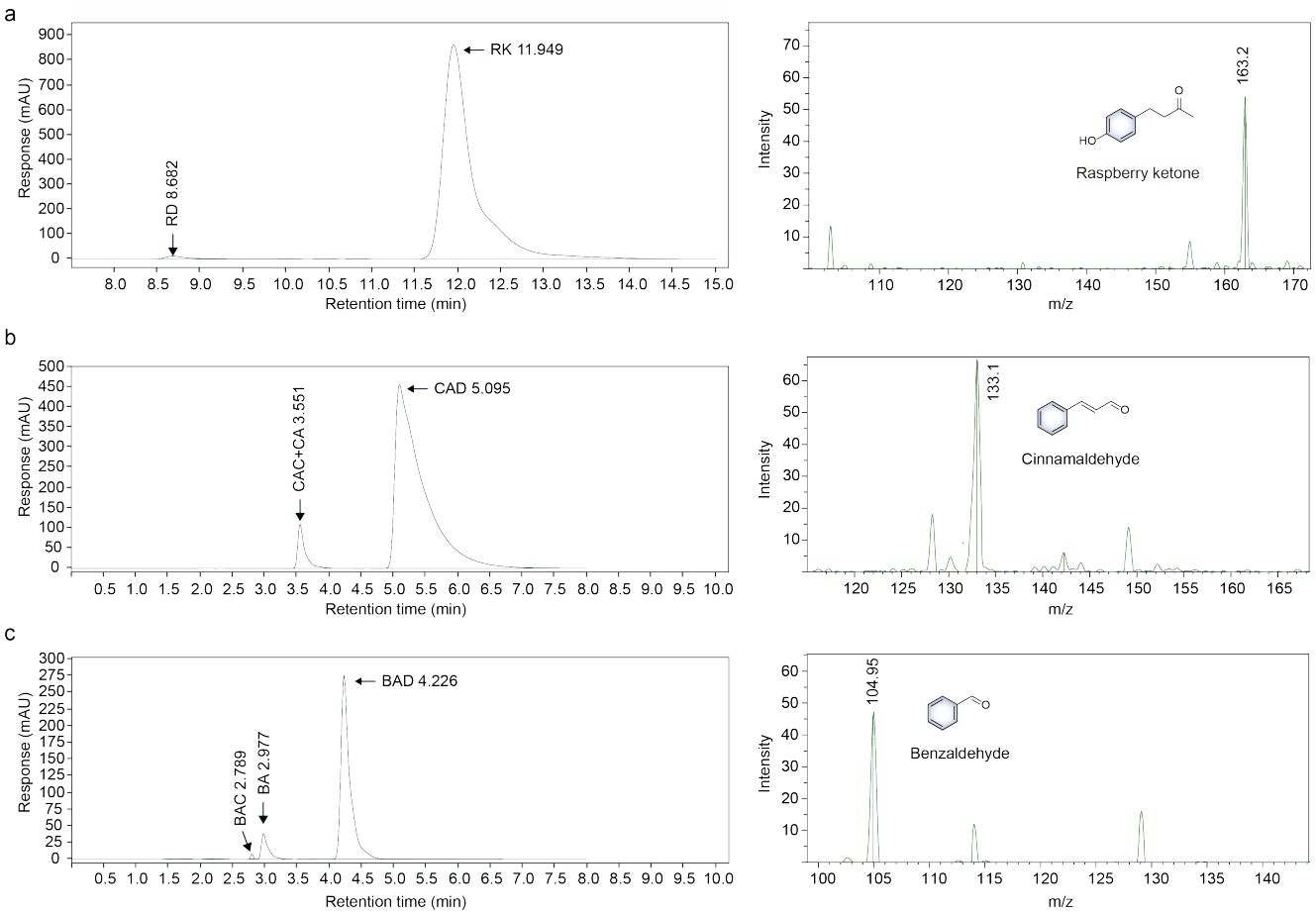

Figure S7. LC-MS/MS analysis of the products. (a) LC-MS/MS analysis of the RK (raspberry ketone) synthesized from rhododendrol (RD) and 4-hydroxybenzylideneacetone (4HBA). The retention time of RK is 11.949 min, with the negative ion mass spectrometry data recorded at m/z = 163.2. (b) LC-MS/MS analysis of the cinnamaldehyde (CAD) synthesized from cinnamyl alcohol (CAC) and cinnamic acid (CA). The retention time of cinnamaldehyde is 5.095 min, with the positive ion mass spectrometry data recorded at m/z = 133.1. (c) LC-MS/MS analysis of the benzaldehyde (BAD) synthesized from benzyl alcohol (BAC) and benzoic acid (BA). The retention time of benzaldehyde is 4.226 min, with the negative ion mass spectrometry data recorded at m/z = 104.95.

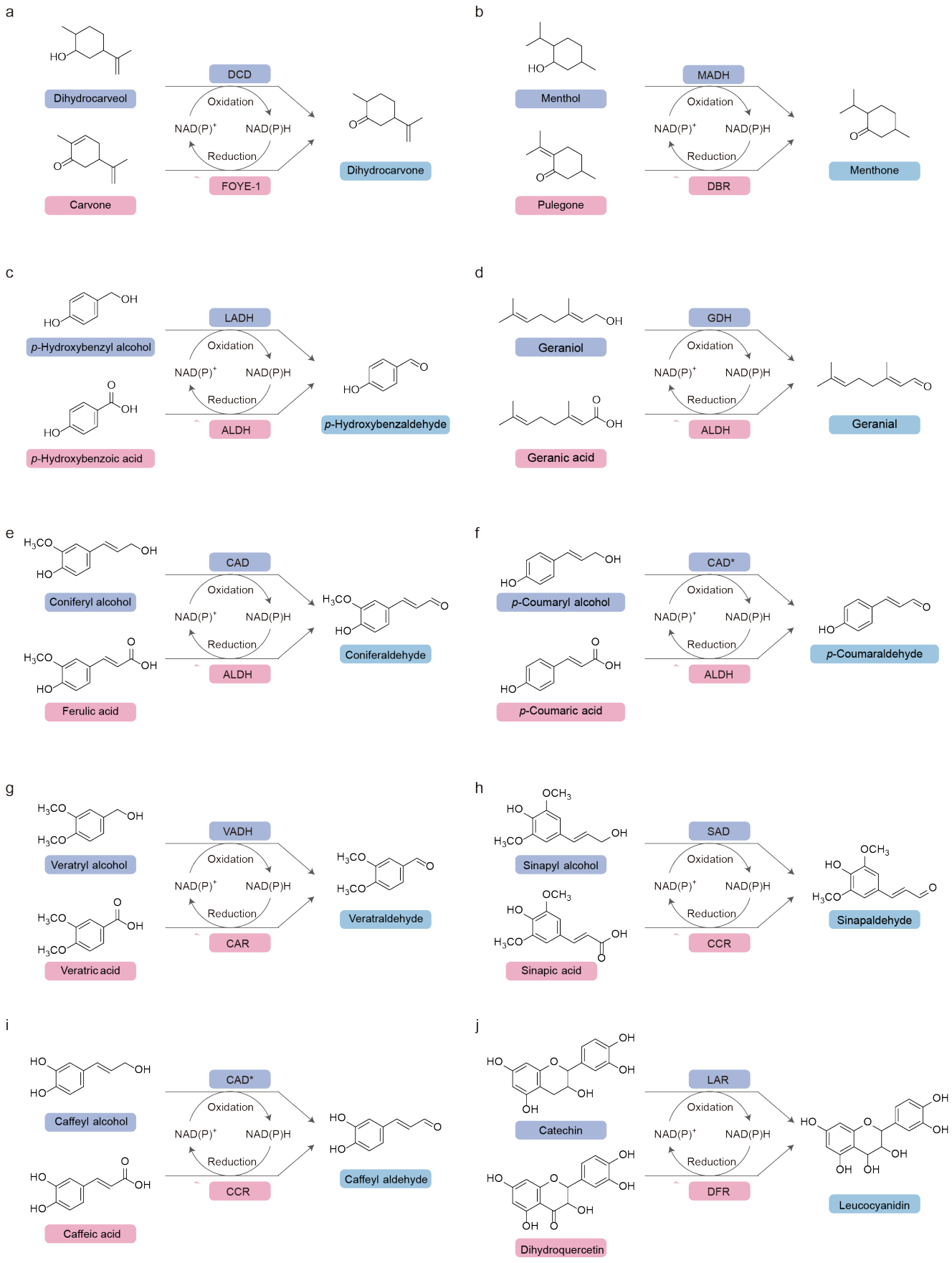

Figure S8. Natural products are potentially synthesized using the MSCR strategy. (a) Conversion of dihydrocarveol and carvone to dihydrocarvone. (b) Conversion of menthol and pulegone to menthone. (c) Conversion of *p*-Hydroxybenzyl alcohol and *p*-hydroxybenzoic

acid to *p*-hydroxybenzaldehyde. (d) Conversion of geraniol and geranic acid to geranial. (e) Conversion of coniferyl alcohol and ferulic acid to coniferaldehyde. (f) Conversion of *p*-coumaryl alcohol and *p*-coumaric acid into *p*-coumaraldehyde. (g) Conversion of veratryl alcohol and veratric acid to veratraldehyde. (h) Conversion of sinapyl alcohol and sinapic acid to sinapaldehyde. (i) Conversion of caffeyl alcohol and caffeic acid to caffeyl aldehyde. (j) Conversion of catechin and dihydroquercetin to leucocyanidin. DCD, Dihydrocarveol dehydrogenase; FOYE-1, Ene-reductases of the Old Yellow Enzyme family (OYEs); MADH, Menthol dehydrogenase; DBR, Double bond reductase; LADH, Liver alcohol dehydrogenase; ALDH, Aldehyde dehydrogenase; GDH, Geraniol dehydrogenase; CAD, Coniferyl alcohol dehydrogenase; CAD*, Cinnamyl alcohol dehydrogenases; VADH, Veratryl alcohol dehydrogenase; CAR, Carboxylic acid reductase; SAD, Sinapyl alcohol dehydrogenase; CCR, Cinnamoyl-CoA reductase; LAR, Leucoanthocyanidin reductase; DFR, Dihydroflavonol 4-reductase.

D. Supporting Tables

Table S1. Plasmids used in this study.

Plasmid	Derivation, relevant characteristics	Source
pETDuet-1	f1 ori, lacI, AmpR, T7 promoter	Lab stock
pET-*Lk*ADH	pETDuet-1 contained the *Lk*ADH gene	This study
pET-*Ai*RZS	pETDuet-1 contained the *Ai*RZS gene	This study
pET-*Oc*RZS	pETDuet-1 contained the *Oc*RZS gene	This study
pET-*Am*ADH1E	pETDuet-1 contained the *Am*ADH1E gene	This study
pET-*Cs*ADH1E	pETDuet-1 contained the *Cs*ADH1E gene	This study
pET-*Am*ADH1E^{4m}	pETDuet-1 contained the *Am*ADH1E^{4m} gene	This study
pET-*Cs*ADH1E^{4m}	pETDuet-1 contained the *Cs*ADH1E^{4m} gene	This study
pET-*Am*ADH1E^{m}	pETDuet-1 contained the *Am*ADH1E^{m} gene	This study
pRSF-*Pa*ADH	pRSFDuet-1 contained the *Pa*ADH gene	This study
pRSF-*Ni*CAR	pRSFDuet-1 contained the *Ni*CAR gene	This study
pRSF-*Bs*SFP	pRSFDuet-1 contained the *Bs*SFP gene	This study
pRSF-*Aa*ADH	pRSFDuet-1 contained the *Aa*ADH gene	This study
pRSF-*Gt*ALDH	pRSFDuet-1 contained the *Gt*ALDH gene	This study

Table S2. Strains used in this study.

Strain	Derivation, relevant characteristics	Source
E.coli Top10	Cloning host	Lab stock
E. coli BL21 (DE3)	Expression host	Lab stock
BL21 (pET-*Lk*ADH)	*E. coli* BL21(DE3) harboring pET-*Lk*ADH	This study
BL21 (pET-*Ai*RZS)	*E. coli* BL21(DE3) harboring pET-*Ai*RZS	This study
BL21 (pET-*Oc*RZS)	*E. coli* BL21(DE3) harboring pET-*Oc*RZS	This study
BL21 (pET-*Am*ADH1E)	*E. coli* BL21(DE3) harboring pET-*Am*ADH1E	This study
BL21 (pET-*Cs*ADH1E)	*E. coli* BL21(DE3) harboring pET-*Cs*ADH1E	This study
BL21 (pET-*Am*ADH1E^{4m})	*E. coli* BL21(DE3) harboring pET-*Am*ADH1E^{4m}	This stud
BL21 (pET-*Cs*ADH1E^{4m})	*E. coli* BL21(DE3) harboring pET-*Cs*ADH1E^{4m}	This study
BL21 (pET-*Am*ADH1E^{m})	*E. coli* BL21(DE3) harboring pET-*Am*ADH1E^{m}	This study
BL21 (pRSF-*Pa*ADH)	*E. coli* BL21(DE3) harboring pRSF-*Pa*ADH	This study
BL21 (pRSF-*Ni*CAR)	*E. coli* BL21(DE3) harboring pRSF-*Ni*CAR	This study
BL21 (pRSF-*Bs*SFP)	*E. coli* BL21(DE3) harboring pRSF-*Bs*SFP	This study
BL21 (pRSF-*Aa*ADH)	*E. coli* BL21(DE3) harboring pRSF-*Aa*ADH	This study
BL21 (pRSF-*Gt*ALDH)	*E. coli* BL21(DE3) harboring pRSF-*Gt*ALDH	This study

Amino acid sequence of *Lk*ADH

MTDRLKGKVAIVTGGTLGIGLAIADKFVEEGAKVVITGRHADVGEKAAKSIGGTDVIRFVQHDASDEAGWTKLFDTTEEAFGPV
TTVVNNAGIAVSKSVEDTTTEEWRKLLSVNLDGVFFGTRLGIQRMKNKGLGASIINMSSIEGFVGDPTLGAYNASKGAVRIMSKS
AALDCALKDYDVRVNTVHPGYIKTPLVDDLEGAEEMMSQRTKTPMGHIGEPNDIAWICVYLASDESKFATGAEFVVDGGYTAQ

Amino acid sequence of *Ri*RZS

MASGGEMQVSNKQVIFRDYVTGFPKESDMELTTRSITLKLPQGSTGLLLKNLYLSCDPYMRARMTNHHRLSYVDSFKPGSPIIGY
GVARVLESGNPKFNPGDLVWGFTGWEEYSVITATESLFKIHNTDVPLSYYTGLLGMPGMTAYAGFYEICSPKKGETVYVSAASG
AVGQLVGQFAKLTGCYVVGSAGSKEKVDLLKNKFGFDEAFNYKEEADLDAALRRYFPDGIDIYFENVGGKMLDAVLPNMRPK
GRIAVCGMISQYNLEQPEGVRNLMALIVKQVRMEGFMVFSYYHLYGKFLETVLPYIKQGKITYVEDVVDGLDNAPAALIGLYSG
RNVGKQVVVVSRE

Amino acid sequence of *Ai*RZS

MPQPSDRNRRYVLAERPVGEPTDQTLRLEVTEIPRPGPGQMLLRNEYLSLDPYMRGRMSDAPSYAPPVGIGEVMVGGTVSQVVE
SNLDGFAPGDWVVAFGGWQDYALSDGRGVVNLGRSPKNPSWYLGVLGMPGLTAWAGLTQIGQPRAGETLVVAAASGPVGAT
VGQIGKILGLRVVGIAGGPEKCAHVVDTLGFDACIDHRAPDLAEALKRAVPDGIDIYFENVGGRVFDAVLPLLNTRARVPVCGLI
AQYNATGLPEGPDRLPLLMGHILRKRMTFRGFIVFDDFGHLYPEFARQMTEWVEQGRIRYREEVIEGLEQAPRAFIGLLRGESFG
KRVVRLTA

Amino acid sequence of *Oc*RZS

MASARRIYLAAFPEGMPTTEHLKLEEVPVPAPAEGQVLLRVIYLSLDPYMRGRMSPVRSYASHINPGDTMVGGTVCEVMESRLE
GFAPGDIVLAGAGWQTHALSDGTGLRKLDPARGPLSAALGVLGMPGFTAYAGLLEHGRPKAGETVVVSAASGAVGQVVGQMA
RILGCRAVGVAGAEDKCRYVTETLGFDAAVNYRADFPEQLAAACPDGVDVYFENVGGAVFDAVLPLMNDFGRIPVCGRIAHYN
DSAPPPGPDRLPAAMGLVLTRRLTFRGFLQFDHLDRWEDFMRDMGGWLAEGRVQYREEIVDGLENAVEAFQGLLTGRNRGKL
VIRVGEDPAAR

Amino acid sequence of *Ct*RZS

MTTDLNRRIVLAAHPHGLPTVQDFRLETGPVPEPGPGQVLLRTLWLSLDPYMRNLMEPVGPGYAEPVPLGGTMVGGTVSRVVA
SRHPRYAAGDLVLAQAGWQDYALSDGGDLLPLGDVTPPSLALGGLGMPGFTAYVGLQDIGQPRPGETVVVAAATGAVGQVVG
QLARLHGARAVGIAGGADKCRIAVEELGFDACLDRHDPQWPQHLAAACPDGIDVYFENVGGAVFDAVLPLLNPGARVPVCGFI
AHYNDGAPPPGPDRLPKLTATLLVKRVRMQGFVILDHYGKRYEAFRREMGRWVADGRVRLREARIDGLERAPEAFVDLLRGRH
VGKVVVRVAGG

Amino acid sequence of *Am*ADH1E

MSTAGKVIKCKAAVLWELKKPFSIEEVEVAPPKAHEVRIKMVASGICRSDEHVVNGTIVAPLPLILGHEAAGIVESIGEGVTTVKP
GDKVIPLFTPQCGKCNVCKHPQGNFCLKNDLSTPRGSMQDGTTRFTCRGKPIHHFVSTSTFSQYTVVDEIAVAKIDPASPLEKVCL
IGCGFSTGYGSAVNIAKVTPGSTCAVFGLGGVGLSVIIGCKAAGAARIIGVDINKDKYAKAKEVGATECISPQDYKEPIQDVLKEM
SGGGVDFSFEVIGRLDTMVAALSCCQESYGVSVIVGVPPNSQNLSMNPMLLLTGRTWKGAIFGGFKSKDSVPKLVADFMAKKFP
LDPLITHVLPFEKINEGFDLLRSGKSIRTILTF

Amino acid sequence of *Am*ADH1E^{m}

MSTAGKVIKCKAAVLWELKKPFSIEEVEVAPPKAHEVRIKMVASGICRSDEHVVNGTIVAPLPLILGHEAAGIVESIGEGVTTVKP
GDKVIPLFTPQCGKCNVCKHPQGNFCLKNDLSTPRGSMQDGTTRFTCRGKPIHHFVSTSTFSQYTVVDEIAVAKIDPASPLEKVCL
IGCGFSTGYGSAVNIAKVTPGSTCAVFGLGGVGLSVIIGCKAAGAARIIGVAINKDKYAKAKEVGATECISPQDYKEPIQDVLKEM
SGGGVDFSFEVIGRLDTMVAALSCCQESYGVSVIVGVPPNSQNLSMNPMLLLTGRTWKGAIFGGFKSKDSVPKLVADFMAKKFP
LDPLITHVLPFEKINEGFDLLRSGKSIRTILTF

Amino acid sequence of *Am*ADH1E^{4m}

MSTAGKVIKCKAAVLWELKKPFSIEEVEVAPPKAHEVRIKMVASGICRSDEHVVNGTIVAPLPLILGHEAAGIVESIGEGVTTVKP
GDKVIPLFTPQCGKCNVCKHPQGNFCLKNDLSTPRGSMQDGTTRFTCRGKPIHHFVSTSTFSQYTVVDEIAVAKIDPASPLEKVCL
IGCGFSTGYGSAVNIAKVTPGSTCAVFGLGGVGLSVIIGCKAAGAARIIGVARSKRKYAKAKEVGATECISPQDYKEPIQDVLKEM
SGGGVDFSFEVIGRLDTMVAALSCCQESYGVSVIVGVPPNSQNLSMNPMLLLTGRTWKGAIFGGFKSKDSVPKLVADFMAKKFP
LDPLITHVLPFEKINEGFDLLRSGKSIRTILTF

Amino acid sequence of *Cs*ADH1E

MSTAGKVIKCKAAVLWELNKPFSIEEVEVAPPKAHEVRIKMVASGICRSDDHVVSGNLVIPLPVIVGHEAAGIVESIGEGVTTVKP
GDKVIPLFTPQCGKCSVCKHPEGNFCLKNDLSTPRGTMQDGTSRFTCRGKPIHHFLGVSTYSQYTVVDEISVAKIDAASSLEKVCL
IGCGFSTGYGSAVKIAKVTQGSTCAVFGLGGVGLSVIMGCKAAGAARIIGVDINKDKFAKAKEVGATECINPQDYEKPIQEVLKE
MSSGGVDFSFEVIGRLDTMMASLSCCHEAYGVSVIVGVPPDSQNLSVNPMLLLSGRTWKGAIFGGFKSKDSVPKLVADFMAKKF
ALDPLITHVLPFEKINEGFDLLRSGKSLRTILTF

Amino acid sequence of *Cs*ADH1E^{m}

MSTAGKVIKCKAAVLWELNKPFSIEEVEVAPPKAHEVRIKMVASGICRSDDHVVSGNLVIPLPVIVGHEAAGIVESIGEGVTTVKP
GDKVIPLFTPQCGKCSVCKHPEGNFCLKNDLSTPRGTMQDGTSRFTCRGKPIHHFLGVSTYSQYTVVDEISVAKIDAASSLEKVCL
IGCGFSTGYGSAVKIAKVTQGSTCAVFGLGGVGLSVIMGCKAAGAARIIGVAINKDKFAKAKEVGATECINPQDYEKPIQEVLKE
MSSGGVDFSFEVIGRLDTMMASLSCCHEAYGVSVIVGVPPDSQNLSVNPMLLLSGRTWKGAIFGGFKSKDSVPKLVADFMAKKF
ALDPLITHVLPFEKINEGFDLLRSGKSLRTILTF

Amino acid sequence of *Cs*ADH1E^{4m}

MSTAGKVIKCKAAVLWELNKPFSIEEVEVAPPKAHEVRIKMVASGICRSDDHVVSGNLVIPLPVIVGHEAAGIVESIGEGVTTVKP
GDKVIPLFTPQCGKCSVCKHPEGNFCLKNDLSTPRGTMQDGTSRFTCRGKPIHHFLGVSTYSQYTVVDEISVAKIDAASSLEKVCL
IGCGFSTGYGSAVKIAKVTQGSTCAVFGLGGVGLSVIMGCKAAGAARIIGVARSKRKFAKAKEVGATECINPQDYEKPIQEVLKE
MSSGGVDFSFEVIGRLDTMMASLSCCHEAYGVSVIVGVPPDSQNLSVNPMLLLSGRTWKGAIFGGFKSKDSVPKLVADFMAKKF
ALDPLITHVLPFEKINEGFDLLRSGKSLRTILTF

References

1 T. Koeduka, B. Watanabe, S. Suzuki, J. Hiratake, J. Mano and K. Yazaki, *Biochem. Biophys. Res. Commun.* 2011, **412**,104-108.

2 A. Becker, D. Böttcher, W. Katzer, K. Siems, L. Müller-Kuhrt and U. T. Bornscheuer, *Appl. Microbiol. Biotechnol.* 2021, **105**, 4189-4197.

3 A. Weckbecker and W. Hummel, *Biocatal. Biotransform.* 2006, **24**, 380-389.

4 Z. Qiu, X. Liu, J. Yu, Y. Zhao, G. R. Zhao, S. Li, K. Liu, L. Du and L. Ma, *Synth. Syst. Biotechnol.* 2024, **9**, 187-195.

5 C. Li, L. Yin, J. Wang, H. Zheng and J. Ni, *Nat. Synth.* 2023, **2**, 960-971.

6 Y. Gemmecker, A. Winiarska, D. Hege, J. Kahnt, A. Seubert, M. Szaleniec and J. Heider, *Appl. Microbiol. Biotechnol.* 2024, **108**, 410.

7 W. B. Black, S. Saleh, S. Perea, E. Luu, Y. Cui, J. Sun, Z. Wang, S. Lambrecht, S. Awachi, D. Hayworth, A. Wang, C. Chuayiuso, R. Hagerty, P. C. Gilcrease, F. Jiao, Z. He, J. B. Siegel and H. Li, *bioRxiv* 2025, doi: 10.1101/2025.07.28.667276.

8 Y. R. Maghraby, R. M. El-Shabasy, A. H. Ibrahim and H. M. E. S. Azzazy, *ACS omega* 2023, **8**, 5184-5196.

9 A. A. Homaei, R. Sariri, F. Vianello and R. Stevanato, *J. Chem. Biol.* 2013, **6**, 185-205.

10 S. Datta, L. R. Christena and Y. R. S. Rajaram, *3 Biotech.* 2013, **3**, 1-9.

11 C. Garcia-Galan, Á. Berenguer-Murcia, R. Fernandez-Lafuente and R. C. Rodrigues, *Adv. Synth. Catal.* 2013, **353**, 2885-2904.

12 I. Es, J. D. G. Vieira and A. C. Amaral, *Appl. Microbiol. Biotechnol.* 2015, **99**, 2065-2082.

13 M. Razzaghi, A. Homaei, F. Vianello, T. Azad, T. Sharma, A. K. Nadda, R. Stevanato, M. Bilal and H. M. N. Iqbal, *Bioprocess. Biosyst. Eng.* 2022, **45**, 237-256.

14 A. Tarafdar, R. Sirohi, V. K. Gaur, S. Kumar, P. Sharma, S. Varjani, H. O. Pandey, R. Sindhu, A. Madhavan, R. Rajasekharan and S. J. Sim, *Bioresour. Technol.* 2021, **326**, 124771.

15 K. Y. Chook, M. K. Aroua and L. T. Gew, *Ind. Eng. Chem. Res.* 2023, **62**, 10800-10812.

16 E. A. de Lima, F. Mandelli, D. Kolling, J. M. Souza, C. A. de Oliveira Filho, M. R. da Silva, I. L. de Mesquita Sampaio, T. L. Junqueira, M. F. Chagas, J. C. Teodoro, E. R. de Morais and M. T. Murakami, *Bioresour. Technol.* 2022, **364**, 128019.

17 R. Bhattacharya, S. Arora and S. Ghosh, *J. Environ. Manage.* 2024, **358**, 120781.

18 A. M. Kunjapur, Y. Tarasova and K. L. J. Prather, *J. Am. Chem. Soc.* 2014, **136**, 11644-11654.

19 J. Ni, Y. Y. Gao, F. Tao, H. Y. Liu and P. Xu, *Angew. Chem. Int. Ed.* 2018, **57**, 1214-1217.

20 C. S. Jamieson, J. Misa, Y. Tang and J. M. Billingsley, *Chem. Soc. Rev.* 2021, **50**, 6950-7008.

21 S. Pugh, R. McKenna, I. Halloum and D. R. Nielsen, *Metab. Eng. Commun.* 2015, **2**, 39-45.

22 Y. Bai, H. Yin, H. Bi, Y. Zhuang, T. Liu and Y. Ma, *Metab. Eng.* 2016, **35**,138-147.

23 G. Rodriguez and S. Atsumi, *Microb. Cell Fact.* 2012, **11**, 90.

24 M. Gottardi, J. D. Knudsen, L. Prado, M. Oreb, P. Branduardi and E. Boles, *Appl. Microbiol. Biotechnol.* 2017, **101**, 4883-4893.

25 Z. Magomedova, A. Grecu, C. W. Sensen, H. Schwab and P. Heidinger, *J. Biotechnol.* 2016, **221**, 78-90.

26 T. Yu, H. Cui, J. Li, Y. Luo, G. Jiang and H. Zhao, *Science* 2023, **379**, 1358-1363.

27 F. Li, L. Yuan, H. Lu, G. Li, Y. Chen, M. K. M. Engqvist, E. J. Kerkhoven and J. Nielsen, *Nat. Catal.* 2022, **5**, 662-672.

28 J. E. Gado, M. Knotts, A. Y. Shaw, D. Marks, N. P. Gauthier, C. Sander and G. T. Beckham, *Nat. Mach. Intell.* 2025, **7**, 716-729.

29 M. Scherer, S. J. Fleishman, P. R. Jones, T. Dandekar and E. Bencurova, *Front. Bioeng. Biotechnol.* 2021, **9**, 673005.

30 C. Ó'Fágáin, *Enzyme Microb. Technol.* 2003, **33**, 137-149.

31 V. Atıroğlu, A. Atıroğlu and M. Özacar, *Food Chem.* 2024, **448**, 138978.

32 J. C. Y. Wu, C. H. Hutchings, M. J. Lindsay, C. J. Werner and B. C. Bundy, *J. Biotechnol.* 2015, **193**, 83-90.

33 Y. Weng, S. Ranaweera, D. Zou, A. P. Cameron, X. Chen, H. Song and C. X. Zhao, *Food Hydrocolloids* 2023, **137**, 108385.

34 Z. Xu, Y. K. Cen, S. P. Zou, Y. P. Xue and Y. G. Zheng, *Crit. Rev. Biotechnol.* 2020, **40**, 83-98.

35 N. Ghahremani Nezhad, R. N. Z. R. A. Rahman, Y. M. Normi, S. N. Oslan, F. M. Shariff and T. C. Leow, *Appl. Microbiol. Biotechnol.* 2022, **106**, 4845-4866.

36 Y. Xie, J. An, G. Yang, G. Wu, Y. Zhang, L. Cui and Y. Feng, *J. Biol. Chem.* 2014, **289,** 7994-8006.

37 A. C. C. Carlsson, M. R. Scholfield, R. K. Rowe, M. C. Ford, A. T. Alexander, R. A. Mehl and P. S. Ho, *Biochemistry* 2018, **57**, 4135-4147.

38 Z. Wang, S. Chen, Y. Li, Y. Xin, C. Liu, H. Su, H. I. Hamouda, M. A. Balah, Y. Mao, H. Jiang and X. Mao, *J. Agric. Food Chem.* 2026, **74**, 10453-10469.

39 N. Rueda, J. C. S. Dos Santos, C. Ortiz, R. Torres, O. Barbosa, R. C. Rodrigues, Á. Berenguer-Murcia and R. Fernandez-Lafuente, *Chem. Rec.* 2016, **16**, 1436-1455.

40 S. Danait-Nabar and R. S. Singhal, *Bioprocess. Biosyst. Eng.* 2023, **46**, 645-664.

41 X. Cai, X. Shi, J. Y. Wang, C. H. Hu, J. D. Shen, B. Zhang, Z. Q. Liu and Y. G. Zheng, *J. Agric. Food Chem.* 2024, **72**, 13186-13195.

42 S. F. Li, F. Cheng, Y. Wang and Y. G. Zheng, Strategies for tailoring pH performances of glycoside hydrolases. *Crit. Rev. Biotechnol.* 2023, **43**, 121-141.

43 M. F. Khan, *World J. Microbiol. Biotechnol.* 2025, **41**, 362.

44 J. Abramson, J. Adler, J. Dunger, R. Evans, T. Green, A. Pritzel, O. Ronneberger, L. Willmore, A. J. Ballard, J. Bambrick, S. W. Bodenstein, D. A. Evans, C. C. Hung, M. O'Neill, D. Reiman, K. Tunyasuvunakool, Z. Wu, A. Žemgulytė, E. Arvaniti, C. Beattie, O. Bertolli, A. Bridgland, A. Cherepanov, M. Congreve, A. I. Cowen-Rivers, A. Cowie, M. Figurnov, F. B. Fuchs, H. Gladman, R. Jain, Y. A. Khan, C. M. R. Low, K. Perlin, A. Potapenko, P. Savy, S. Singh, A. Stecula, A. Thillaisundaram, C. Tong, S. Yakneen, E. D. Zhong, M. Zielinski, A. Žídek, V. Bapst, P. Kohli, M. Jaderberg, D. Hassabis and J. M. Jumper, *Nature*, 2024, **630**, 493-500.

45 H. Wang, T. Fu, Y. Du, W. Gao, K. Huang, Z. Liu, P. Chandak, S. Liu, P. van Katwyk, A. Deac, A. Anandkumar, K. Bergen, C. P. Gomes, S. Ho, P. Kohli, J. Lasenby, J. Leskovec, T. Y. Liu, A. Manrai, D. Marks, B. Ramsundar, L. Song, J. Sun, J. Tang, P. Veličković, M. Welling, L. Zhang, C. W. Coley, Y. Bengio and M. Zitnik, *Nature* 2023, **620**, 47-60.

46 Z. Lin, H. Akin, R. Rao, B. Hie, Z. Zhu, W. Lu, N. Smetanin, R. Verkuil, O. Kabeli, Y. Shmueli, A. dos Santos Costa, M. Fazel-Zarandi, T. Sercu, S. Candido and A. Rives, *Science* 2023, **379**, 1123-1130.

47 M. J. van der Werf and A. M. Boot, *Microbiology* 2000, **146**, 1129-1141.

48 D. Tischler, E. Gädke, D. Eggerichs, A. Gomez Baraibar, C. Mügge, A. Scholtissek and C. E. Paul, *ChemBioChem* 2020, **21**, 1217-1225.

49 R. Kjonaas, C. Martinkus-Taylor and R. Croteau, *Plant Physiol.* 1982, **69**, 1013-1017.

50 D. J. Mansell, H. S. Toogood, J. Waller, J. M. Hughes, C. W. Levy, J. M. *ACS Catal.* 2013, **3**, 370-379.

51 C. C. Wratten and W. W. Cleland, *Biochemistry* 1965, **4**, 2442-2451.

52 Y. Iijima, T. Koeduka, H. Suzuki and K. Kubota, *Plant Biotechnol.* 2014, **31**, 525-534.

53 R. L. Mansell, G. R. Babbel and M. H. Zenk, *Phytochemistry* 1976, **15**, 1849-1853.

54 M. Varbanova, K. Porter, F. Lu, J. Ralph, R. Hammerschmidt, A. D. Jones and B. Day, *Plant Physiol.* 2011, **157**, 1056-1066.

55 E. de Jong, E. E. Beuling, R. P. van der Zwan and J. A. M. de Bont, *Appl. Microbiol. Biotechnol.* 1990, **34**, 420-425.

56 M. Winkler and J. G. Ling, *ChemCatChem* 2022, **14**, e202200441.

57 L. Li, X. F. Cheng, J. Leshkevich, T. Umezawa, S. A. Harding and V. L. Chiang, *Plant Cell* 2001, **13**, 1567-1586.

58 V. Lauvergeat, C. Lacombe, E. Lacombe, E. Lasserre, D. Roby and J. Grima-Pettenati, *Phytochemistry* 2001, **57**, 1187-1195.

59 S. J. Kim, M. R. Kim, D. L. Bedgar, S. G. A. Moinuddin, C. L. Cardenas, L. B. Davin, C. Kang and N. G. Lewis, *Proc. Natl. Acad. Sci. U. S. A.* 2001, **101**, 1455-1460.

60 R. Zhou, L. Jackson, G. Shadle, J. Nakashima, S. Temple, F. Chen, and R. A. Dixon, *Proc. Natl. Acad. Sci. U. S. A.* 2010, **107**, 17803-17808.

61 J. A. Chemler, Z. L. Fowler, K. P. McHugh and M. A. G. Koffas, *Metab.Eng.* 2010, **12**, 96-104.